

# Thermodynamic analysis of Jun–Fos coiled coil peptide antagonists

## Inferences for optimization of enthalpic binding forces

Jonathan A. R. Worrall and Jody M. Mason

Department of Biological Sciences, University of Essex, Colchester, UK

### Keywords

activator protein-1; coiled coil; isothermal titration calorimetry; jun-fos; protein design

### Correspondence

J. M. Mason, Department of Biological Sciences, University of Essex, Wivenhoe Park, Colchester CO4 3SQ, UK  
Fax: +44 1206 872592  
Tel: +44 1206 873010  
E-mail: [jmason@essex.ac.uk](mailto:jmason@essex.ac.uk)

(Received 23 August 2010, revised 12 November 2010, accepted 7 December 2010)

doi:10.1111/j.1742-4658.2010.07988.x

Dimerization of the Jun–Fos activator protein-1 (AP-1) transcriptional regulator is mediated by coiled coil regions that facilitate binding of the basic regions to a specific promoter. AP-1 is responsible for the regulation of a number of genes involved in cell proliferation. We have previously derived peptide antagonists and demonstrated them to be capable of binding to the Jun or Fos coiled coil region with high affinity ( $K_D$  values in the low nM range relative to  $\mu\text{M}$  for the wild-type interaction). Use of isothermal titration calorimetry combined with CD spectroscopy is reported to elucidate the thermodynamic parameters that drive the interaction stability of peptide antagonists with their cJun and cFos targets. We observe that the free energy of binding for antagonist–target complexes is dominated by the enthalpic term, is opposed by unfavourable entropic contributions consistent with reduced conformational freedom and that these values in turn correlate well ( $r = -0.97$ ) with the measured helicity of each dimeric pair. The more helical the antagonist–target complex, the more favourable the change in enthalpy, which is in turn opposed more strongly by entropy. Antagonistic peptides are predicted to represent excellent scaffolds for further refinement. By contrast, the wild-type cJun–cFos complex is dominated by a favourable entropic contribution, owing partially to a decrease in buried hydrophobic groups from cFos core residues and an increase in the conformational freedom.

### Structured digital abstract

- [MINT-8077649](#), [MINT-8077677](#), [MINT-8077771](#), [MINT-8077789](#), [MINT-8077811](#), [MINT-8077831](#): *c-Jun* (uniprotkb:[P05412](#)) and *c-Fos* (uniprotkb:[P01100](#)) bind ([MI:0407](#)) by isothermal titration calorimetry ([MI:0065](#))
- [MINT-8077856](#), [MINT-8077872](#), [MINT-8077889](#), [MINT-8077906](#), [MINT-8077923](#), [MINT-8077940](#): *c-Jun* (uniprotkb:[P05412](#)) and *c-Fos* (uniprotkb:[P01100](#)) bind ([MI:0407](#)) by circular dichroism ([MI:0016](#))

## Introduction

The transcriptional regulator activator protein-1 (AP-1) generally consists of heterodimers of the Jun (e.g. cJun, JunB, JunD) and Fos (e.g. cFos, FosB, Fra1, Fra2) families of proteins. Different homologues combine to

form different heterodimers, which in turn have different expression patterns depending on the tissue. AP-1 is responsible for the regulation of a number of key genes that include cyclin D1 and interleukin-2, and is

### Abbreviations

AP-1, activator protein-1; CANDI, competitive and negative design initiative; ITC, isothermal titration calorimetry; PCA, protein-fragment complementation assay; PPI, protein–protein interaction.

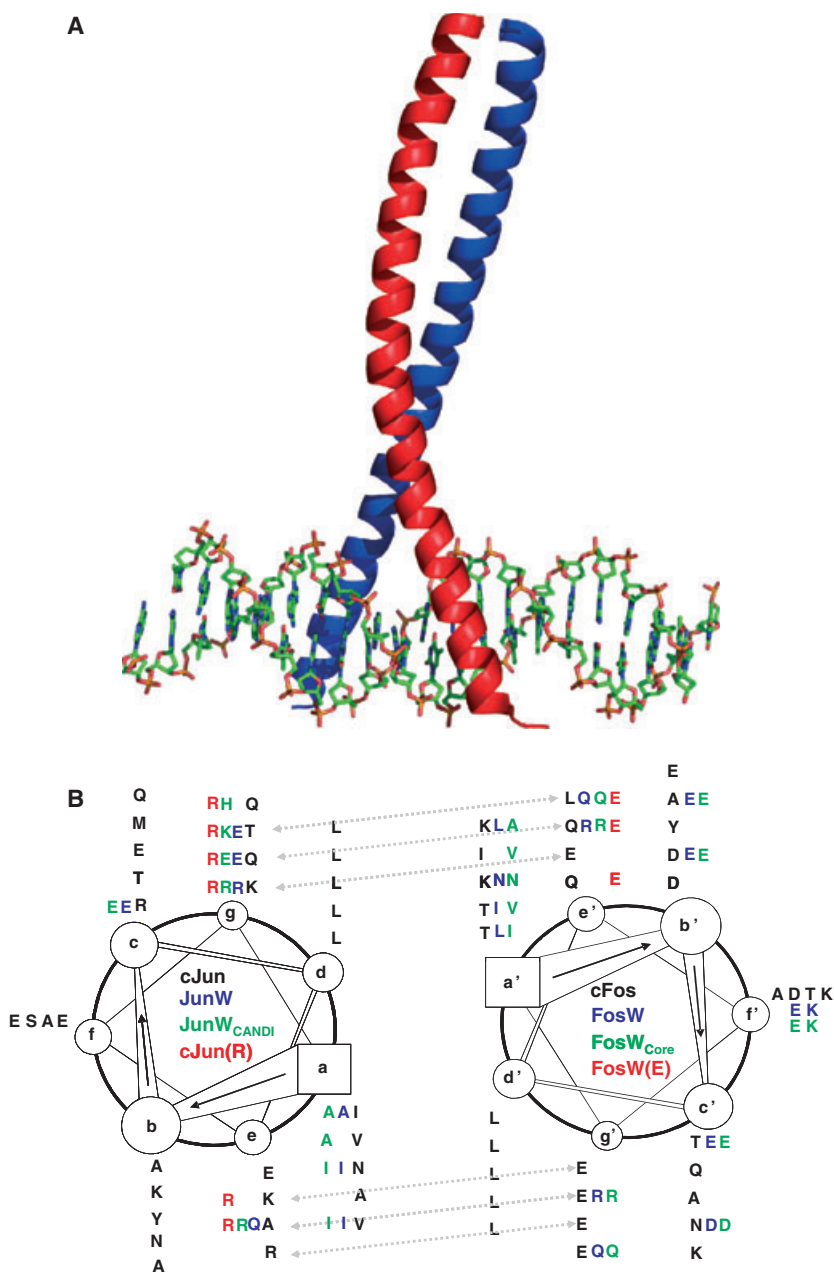


**Fig. 1.** (A) The structure of the native DNA-bound cJun–cFos AP-1 bZIP domain (PDB coordinates 1FOS) [7] containing the bZIP region of the two proteins. cJun is shown in red and cFos in blue. The ‘basic’ N-terminal regions are rich in arginine and lysine and are responsible for scissor gripping the DNA upon recognition of their cognate binding sequence (TGACTCA). C-terminal of this basic region is the leucine zipper (coiled coil) region that is responsible for mediating dimerization of the two chains, and is therefore the focus of this study. The figure created using PYMOL (DeLano Scientific; <http://pymol.sourceforge.net/>). (B) A helical wheel representation highlighting the interaction patterns for the various heterodimers. Residues for cJun (left) and cFos (right) are coloured black. Residues for JunW, JunW<sub>CANDI</sub> and cJun(R) that differ from those of cJun are shown as blue, green and red, respectively. Similarly, residues for FosW, FosW<sub>Core</sub> and FosW(E) that differ from those of cFos are shown as blue, green and red, respectively.

connected to a number of cell signalling cascades. It has consequently been demonstrated that AP-1 upregulation is involved in a number of diseases, including cancer [1–3] bone disease (e.g. osteoporosis) and inflammatory diseases such as rheumatoid arthritis and psoriasis [4–6]. Thus, peptides capable of specifically sequestering key components of AP-1, and that therefore prevent its function, show great promise as the starting point for drugs to combat a number of diseases. The native AP-1 dimer (Fig. 1) consists of a transactivation domain, a basic domain, rich in lysine and arginine residues, that is responsible for mediating

DNA binding and a coiled coil (leucine zipper) region that is known to mediate dimerization of the two chains. Developing rules that can assist in the discovery of new binding partners for coiled-coil-containing proteins therefore has great potential for influencing biology by elucidating stable and specific protein–protein interactions (PPIs) [8]. We have consequently derived several peptides, based upon the coiled coil regions of AP-1, that are able to bind to the corresponding coiled coil regions of key AP-1 homologues and prevent them from binding to DNA via their basic region. Thus, these antagonists have the potential to

sequester these proteins as nonfunctional heterodimers to prevent binding to native partners. The first of these peptides was generated by semirational design using the native binding partner as a scaffold. Degenerate codons important in dimerization were introduced and a protein-fragment complementation assay (PCA) [9,10] was undertaken to screen the resultant library and single out peptide sequences capable of generating an interaction with the target protein. This ensured that only library members that bound to the target generated colonies under selective conditions. Growth competitions then ensured that only those PPIs of highest affinity were enriched. The peptides, JunW and FosW, bound to cFos and cJun, respectively, with much higher interaction stability than the parent protein [11]. In order to increase the specificity of PCA-generated PPIs, we incorporated a competitive and negative design initiative (CANDI) into the screen. CANDI is used to ensure that the energy gap between desired and undesired complexes is maximized and works by including sequences competing for an interaction with either the target and/or the library member in the bacterial selection [12,13]. Library members that bind to the competitor, are promiscuous in their binding selection or cannot compete with the competitor–target complex are subsequently removed from the bacterial pool. Using the PCA–CANDI technique, we generated a peptide, JunW<sub>CANDI</sub>, that is specific for cFos even in the presence of a cJun competitor. This is in sharp contrast to JunW, which binds with high affinity to both cJun and cFos. This study offers the possibility to look at the underlying thermodynamic signature behind these two binding events. Libraries based on the cJun–FosW peptide have also been created with both core and electrostatic semirandomizations. Using competitive growth competitions, it was found that the winner of the core randomization, FosW<sub>Core</sub>, was able to bind to cJun specifically in the presence of competing Fos homologues [14]. The FosW<sub>Core</sub> library was based upon FosW and contained 12 residue options (codon NHT = F, L, I, V, S, P, T, A, Y, H, N or D) at four of five  $\alpha$  position residues. This study reflected the fact that core residues impose large energetic changes, with consequent growth competitions, suggesting that they also have the ability to impart specificity in instances where electrostatic options are insufficient. Finally an electrostatically enhanced dimer, cJun(R)–FosW(E), has been previously studied to dissect the free energy of binding into its component steps, and was found to have achieved increased equilibrium stability as a result of large decrease in the dissociation rate of the complex [15].

## Thermodynamics of binding

To enable us to address the question of a common underlying mechanism by which all of these antagonists achieve high interaction affinity, we decided to use CD data and isothermal titration calorimetry (ITC) to split the free energy of binding into its component parts, the enthalpy ( $\Delta H$ ) and the temperature multiplied by the entropic contribution ( $T\Delta S$ ) according to the relationship:

$$\Delta G_{\text{bind}} = \Delta H - T\Delta S \quad (1)$$

Where a negative  $\Delta G_{\text{bind}}$  value represents a spontaneous reaction that is favourable,  $\Delta H$  represents the strength of the target–antagonist complex relative to those of the solvent and includes electrostatic bonds, van der Waal's interactions and hydrogen bond formation. A negative  $\Delta H$  value is representative of a favourable enthalpic contribution to the reaction. By contrast, a positive  $T\Delta S$  value represents a favourable entropic contribution. Favourable entropy can come from hydrophobic interactions that release water molecules upon their formation as well as minimal loss in conformational freedom. Although binding affinity can be optimized by either enthalpic or entropic improvements, so long as they are not compensated for by opposite entropic or enthalpic changes [16,17], optimization of the binding energy via a negative enthalpic term is favoured. However, optimizing noncovalent bonds is extremely difficult to achieve by rational design, because it is often accompanied by entropy compensation. By studying a range of antagonists that have been designed or selected by enriching the highest affinity binding partners from libraries that target cJun and cFos, it is anticipated that we can split the free energy of binding into its thermodynamic components to investigate whether there is a thermodynamic profile that is common to all of these molecules.

## Results

We used ITC to extract the thermodynamic parameters that make up the overall free energy of binding ( $\Delta G_{\text{bind}}$ ) for our antagonist–peptide complexes. The antagonists (see Table 1 for sequences and Fig. 2 for example ITC profiles) have previously been shown to be capable of sequestering cJun or cFos using a variety of techniques, including CD thermal denaturation studies [11,12,20], kinetic folding studies [15,21] and native gel analysis [12,15]. We observe that the enthalpic component is strongly favoured for our antagonist–target complexes and that the change in entropy is unfavourable. However, in contrast to Seldeen *et al.* [18], we observe that

**Table 1.** Peptide sequences and the sequences used by Seldeen *et al.* [18], which lack N and C capping motifs and contain an 11.7 kDa thioredoxin motif fused to the N-terminus and a hexahistidine tag at the C-terminus, separated by thrombin cleavage sites.

Name	Sequence				
	abcde	fg	abcde	fg	abcde
cJun	AS	IARLEEK	VKTLKAE	NYELAST	ANMLREQ
cFos	AS	TDTLQAE	TDQLEDE	KYALQTE	IANLLKE
FosW	AS	LDELQAE	IEQLEER	NYALRKE	IEDLQKQ
JunW	AS	AAELEER	VKTLKAE	IYELQSE	ANMLREQ
JunW <sub>CANDI</sub>	AS	AAELEER	AKTLKAE	IYELRSK	ANMLREH
FosW <sub>Core</sub>	AS	IDELQAE	VEQLEER	NYALRKE	VEDLQKQ
cJun(R)	AS	IARLRER	VKTLRAR	NYELRSR	ANMLRER
FosW(E)	AS	LDELEAE	IEQLEEE	NYALEKE	IEDLEKE
LZ (cJun) <sup>a</sup>	Trx-	IARLEEK	VKTLKAE	NSELAST	ANMLREQ
LZ (cFos) <sup>a</sup>	Trx-	TDTLQAE	TDQLEDE	KSALQTE	IANLLKE

<sup>a</sup> Seldeen *et al.* [18,19] generated 28mers with peptides fused to an 11.7 kDa N-terminal thioredoxin (Trx) tag to assist with solubility and expression, as well as a C-terminal (His)<sub>6</sub>-tag. Both tags were additionally separated by thrombin sites (LVPRGS) which upon cleavage caused significant destabilization of the peptides. Their experimental conditions (50 mM Tris, 200 mM NaCl, 1 mM EDTA and 5 mM  $\beta$ -mercaptoethanol at pH 8) varied from this study.

the overall free energy of binding for the wild-type leucine zipper complex is driven by a strong entropic component. Moreover, as is the case for the parent AP-1 leucine zipper, our antagonists are predicted to form a helical structure that gives rise to a coiled coil with either the cJun or cFos target peptide. This structure is maintained by core hydrophobic interactions, primarily brought about by knobs into holes packing between a-a' and d-d' residues, and from which the bulk of stability arises. In addition, flanking electrostatic interactions between g-e' + 1 core flanking residues are speculated to play a primary role in specificity [22,23]. Together, both of these types of interaction are predicted to give rise to a favourable enthalpic transition upon binding. By contrast, the entropic term is largely dominated by the net result of two opposing forces. The first, conformational entropy ( $\Delta S_{\text{conf}}$ ) results in a positive (unfavourable) net contribution to the overall free energy of binding.  $\Delta S_{\text{conf}}$  arises from a reduction in conformational degrees of freedom of backbone and side chain atoms as the molecule folds and gains structure. By contrast, desolvational entropy ( $\Delta S_{\text{solv}}$ ) contributes favourably to the net free energy of binding and results from the release of water molecules bound to regions of the target and antagonist that become buried in fully formed complex.

### Wild-type Jun-Fos leucine zipper region

The native coiled coil region of this human transcriptional regulator produces a relatively weak interaction, as has been well documented [11,12,21]. Addition of DNA and other factors such as disulfide bridges [24,25] and additional flanking regions [18,26–28] have been shown to increase the stability of the complex. In

this analysis, however, we have focused entirely on the unmodified coiled coil region of the wild-type AP-1 protein. This coiled coil dimerization motif is 4.5 heptads in length. We find that the free energy of binding is driven predominantly by a favourable entropy ( $T\Delta S$ ; 5.32 kcal·mol<sup>-1</sup>), with only a very small enthalpic contribution ( $\Delta H$ ; -0.82 kcal·mol<sup>-1</sup>) to binding at 293 K. The favourable entropy term arises mainly from desolvation effects which outweigh the unfavourable conformational penalty. This is consistent with an observed weak enthalpic contribution to the free energy of binding. Indeed, the free energy of binding is 2–3 kcal·mol<sup>-1</sup> less than any of the antagonist-cJun or antagonist-cFos complexes. ITC data collected from the leucine zipper region of cJun and cFos correlate poorly with the findings of Seldeen *et al.* [18] (see Tables 1 and 2). We believe that their data overestimate the free energy of binding for the leucine zipper region in the absence of DNA. One possibility could be the use of a fusion construct with a (His)<sub>6</sub>-tag and Trx-tag included to necessitate purification and solubility of the cJun/cFos leucine zippers. Seldeen *et al.* noted that these additional units were not anticipated to interact with the bZIP domains of Jun and Fos.

Our ITC data on the stability of the cJun-cFos interaction correlate well with thermal melting data (see Table 2 and [11]), chemical denaturation data [12] and earlier studies that have probed these regions [11] (and references therein). In addition, both the bZIP coiled coil prediction algorithm and the base-optimized weights method of *in silico* coiled coil stability prediction anticipate the measured stability of all of our coiled coils pairs with reasonable accuracy, giving us confidence in the reliability of our data. In addition,

**Table 2.** Thermodynamic data from ITC, thermal melting analysis and bZIP  $K_D$  values are shown as derived using ITC data, and in parentheses from data taken using the midpoint of the transition from thermal denaturation profiles (and fit as temperature as a function of  $\ln K_D$ , with the fit  $\ln K_D = aT + C$  where  $a$  is the gradient,  $T$  is the temperature in Celsius and  $C$  is the intercept) and calculated at 20 °C. Note that Seldeen's data were collected at 25 °C, although data were also collected at 20 °C and show entropy–enthalpy compensation; a lowering of the contribution made by  $\Delta H$  (from –23 to approximately –18) is compensated for by a reduction in the contribution from  $T\Delta S$  (from –13.5 to approximately –8), resulting in almost no overall change in  $\Delta G_{\text{bind}}$  (–9.7 to approximately –10). A = data obtained using van't Hoff plots extracted from thermal melts and extrapolated to 20 °C. N/A, not available.

	cJun–cFos [18]	cJun–cFos	cJun–FosW	cJun–FosW <sub>Core</sub>	cFos–JunW	cFos–JunW <sub>CANDI</sub>	cJun(R)–FosW(E)
N	N/A	1.06 (0.01)	0.65 (0.01)	0.95 (0.01)	0.69 (0.01)	0.80 (0.01)	0.78 (0.01)
$K_B$ (M <sup>−1</sup> )	$1.6 \times 10^7$	$3.76 \times 10^4$ ( $2.54 \times 10^4$ )	$2.21 \times 10^7$ ( $4.28 \times 10^6$ )	$7.9 \times 10^5$ ( $3.86 \times 10^4$ )	$1.26 \times 10^6$ ( $9.15 \times 10^4$ )	$8.31 \times 10^5$ ( $3.97 \times 10^4$ )	$1.45 \times 10^7$ ( $2.37 \times 10^5$ )
$\Delta H$ (kcal·mol <sup>−1</sup> )	−23.21 (0.23)	−0.82 (0.36)	−10.55 (0.16)	−11.94 (0.14)	−13.9 (0.24)	−14.8 (0.25)	−27.0 (0.40)
$T\Delta S$ (kcal·mol <sup>−1</sup> ) [ $\Delta H - \Delta G$ ]	−13.52 (0.42)	5.32 (0.53)	−0.68 (0.19)	−4.03 (0.14)	−5.72 (0.24)	−6.86 (0.25)	−17.4 (0.41)
$\Delta G_{\text{bind}}$ ITC (kcal·mol <sup>−1</sup> )	−9.69 (0.26)	−6.14 (0.39)	−9.87 (0.11)	−7.91 (0.03)	−8.18 (0.04)	−7.94 (0.03)	−9.60 (0.10)
$K_D$ 20 °C ITC (M <sup>−1</sup> thermal)	60 nM (25 °C) (N/A)	26.6 $\mu$ M (324 $\mu$ M)	45 nM (4 nM)	1.27 $\mu$ M (20 $\mu$ M)	0.79 $\mu$ M (40 $\mu$ M)	1.2 $\mu$ M (0.45 $\mu$ M)	69 nM (0.15 nM)
$\Delta G$ thermal (kcal·mol <sup>−1</sup> ) <sup>a</sup>	N/A	−5.5	−11.4	−8.6	−8.1	−8.5	−18.0
Measured $T_m$	N/A	16	63	45	44	44	98 <sup>a</sup>
bCIPA $T_m$ <sup>b</sup>	25	13	62	56	37	49	90
BOW <sup>c</sup>	N/A	26.9	41.4	35.1	33.4	33.4	55.6

<sup>a</sup> Extrapolated from fit using a restrained upper baseline based on alternative dimer thermal denaturation profiles. <sup>b</sup> Predicted thermal melting value based on sequence data using basic coiled coil interaction algorithm (bCIPA). <sup>c</sup> Predicted interaction score according to base optimized weights (BOWs) [29].

**Table 3.** Helical calculations to assist in establishing whether the peptide is representative of a coiled coil structure [30–32].

Peptides (150 $\mu$ M Pt)	$\theta_{222}/\theta_{208}$	Fraction helical ( $f_H$ )	Averaged helicity in % predicted by Agadir (293 K)
cJun	0.53	14.6	3.7
cFos	0.65	17.3	3.5
FosW	1.02	43.7	26.2
JunW	1.01	41.7	17.0
JunW <sub>CANDI</sub>	0.79	22.2	21.9
FosW <sub>Core</sub>	0.74	26.6	10.2
cJun(R)	0.54	22.3	4.8
FosW(E)	0.45	17.2	7.9
cJun–cFos	0.75	25.0	3.6
cJun–FosW	1.00	40.0	15.0
cJun–FosW <sub>Core</sub>	0.91	43.1	7.0
cFos–JunW	1.00	45.7	10.3
cFos–JunW <sub>CANDI</sub>	0.97	48.4	12.7
cJun(R)–FosW(E)	1.00	88.0	6.4

The  $\theta_{222}/\theta_{208}$  ratios provide information on the likelihood of the alpha-helix being in isolation or being found within a coiled coil structure [30,31,33]. A ratio  $> 1.0$  typically indicates the latter, whereas a ratio of  $\sim 0.9$  or less indicates the presence of a helix in isolation. For all dimeric pairs, except the wild-type structure (which is known to interact with low affinity), the ratio is  $> 0.9$ , supporting the formation of a coiled coil structure. Fraction helicity ( $f_H$ ) can be calculated as  $f_H = (\theta_{222} - \theta_c)/(\theta_{222\infty} - \theta_c)$ , where  $\theta_{222\infty} = (-44000 + 250T) \times (1 - k/Nr)$  and  $\theta_c = 2220 - (53 \times T)$ . In these equations the wavelength-dependent constant  $k = 2.4$  (at 222 nm),  $Nr$  = the number of residues and  $T = 20$  °C (293 K). Agadir [34–36] severely underestimates helicity for many of the dimeric pairs, most likely because it does not take into account the interhelical interactions that assist with helix integrity in the dimeric pairs; it considers only the helicity of individual helices in isolation. Thus, the measured helicity is often higher than the values predicted from the average of the two constituent helices by Agadir. Indeed, in the most extreme case, cJun(R)–FosW(E), interhelical electrostatics are particularly prominent. When not considered, these  $e/g$  interactions would be grossly underestimated as merely the average of the two isolated constituent helices (6.4%). However, at 88% measured helicity, this ER pair associates to form the most helical and indeed most stable coiled coil interaction in this study.

the comparatively low level of helicity (both measured and predicted) for cJun, cFos and cJun–cFos (see Table 3) supports the notion that this wild-type interaction is relatively modest in stability. Collectively, previous studies on cJun–cFos leucine zipper pairs have implied an interaction that is unstable ( $T_m = 16$  °C [11],  $\Delta G_{\text{bind}} = 5.5$  kcal·mol<sup>−1</sup> [21]) at physiological temperatures, which is considered important in ensuring that the transcription factor is not constitutively active *in vivo*. Rather, weak binding permits the complex to extend its helicity into the basic regions while either binding to or dissociating from the DNA.

### Peptides designed to target cJun

FosW and FosW<sub>Core</sub> have both been designed to target the cJun peptide. Both form dimeric complexes with cJun that are much more stable than wild-type ( $\Delta G_{\text{bind}} = -9.9$  and  $-7.9$  kcal·mol<sup>-1</sup> relative to  $-6.1$  kcal·mol<sup>-1</sup>). For both antagonists, the majority of this increased interaction stability is the result of a favourable enthalpy ( $-10.6$  and  $-11.9$  kcal·mol<sup>-1</sup> relative to  $-0.82$  kcal·mol<sup>-1</sup>; see Table 2), with the entropic component opposing the binding process. Although FosW has 2 kcal·mol<sup>-1</sup> more interaction stability for cJun relative to FosW<sub>Core</sub>, and its enthalpic contribution is 1.4 kcal·mol<sup>-1</sup> less, the entropic penalty is  $> 3$  kcal·mol<sup>-1</sup> less. Therefore the interaction is more stable. The fact that the entropic term is much less unfavourable than for cJun–FosW<sub>Core</sub> agrees well with the predicted helical propensity of FosW and FosW<sub>Core</sub>; both the measured helicity (taken using the 222 signal and expressed as a fraction of maximal potential helicity according to Hodges and co-workers [30,31] and Shepherd *et al.* [33]), and calculated helicity according to Agadir [34–36] predicts that FosW<sub>Core</sub> has approximately half the average helical content of FosW at 293 K [15,34–36]. However, upon binding to cJun, both heterodimeric pairs display similar measured helicity, suggesting that for cJun–FosW,  $\Delta S_{\text{conf}}$  and  $\Delta S_{\text{solv}}$  almost cancel each other out. However, when FosW<sub>Core</sub> binds cJun, the entropic contribution disa-

vours the overall interaction stability. There is very little increase in the predicted helicity of subunits upon binding, suggesting that desolvation effects are outweighed by conformational entropy for this pair. By contrast, for cJun–FosW, which has similar measured helicity but very little unfavourable entropy, conformational entropy is likely to be comparable but with increased desolvational entropy contributions. Thus, residual water molecules, possibly resulting from an additional alanine residue in the core region of the cJun–FosW<sub>Core</sub> complex, may be responsible for generating a more unfavourable  $\Delta S_{\text{solv}}$ , although a strong overall enthalpic term is maintained. This is consistent with a library in which four of the five  $\alpha'$  positions were selected from twelve residue options [14] to give an improved enthalpy of binding, over FosW.

### Peptides designed to target cFos

JunW and JunW<sub>CANDI</sub> have both been selected using PCA, but the latter has been generated to bind cFos with increased specificity in the presence of a cJun competitor, thus rendering the interaction stable and specific [12]. Analysis of the ITC data informs that, in agreement with thermal denaturation data, there is almost no change in the free energy of binding. However, dissection of this value into its thermodynamic components reveals JunW<sub>CANDI</sub> to have a slight increase in enthalpy change upon binding cFos ( $-14.8$

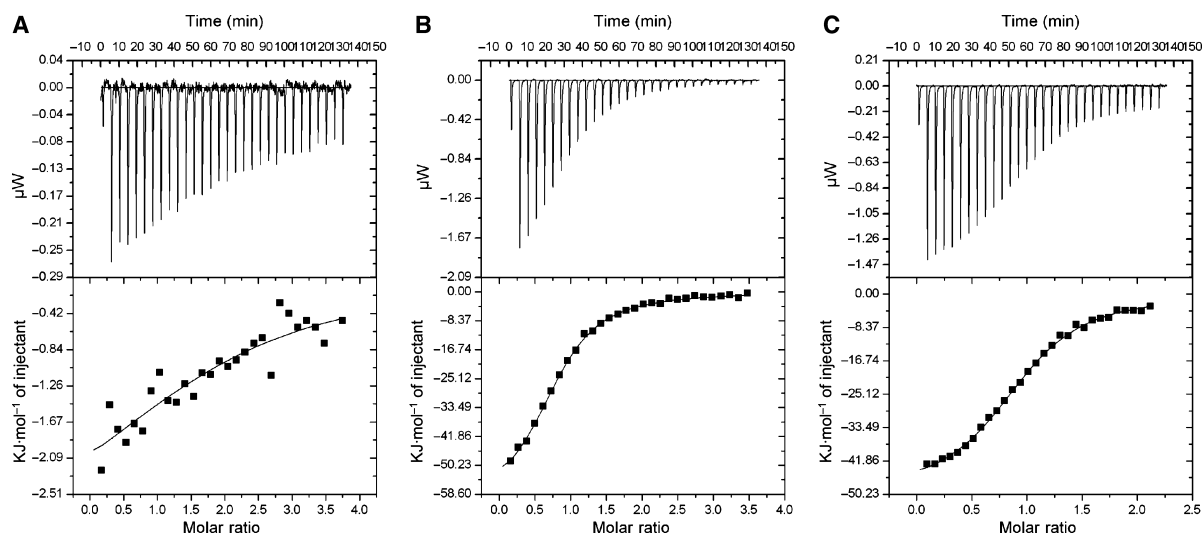


**Fig. 2.** Isothermal titration calorimetry (ITC) analysis of leucine zipper domain interactions between cJun and cFos, as well as their interaction with peptide antagonist. (A) cFos into cJun, (B) cFos into JunW<sub>CANDI</sub> and (C) cJun into FosW<sub>Core</sub>. The upper and lower panels show raw data and data after baseline correction, respectively. During ITC experiments,  $\sim 200$ – $600$   $\mu\text{M}$  of peptide A was injected in  $30$ – $40 \times 5$   $\mu\text{L}$  batches from the injection syringe into the cell, which contained  $10$ – $40$   $\mu\text{M}$  peptide B. Both partners were in a  $10$  mM potassium phosphate buffer,  $100$  mM potassium fluoride at pH 7. Experiments were undertaken at  $20$  °C. The solid lines represent the fit of the data to the function based on the binding of a ligand to a macromolecule using Microcal (GE Healthcare, Uppsala, Sweden) ORIGIN software [39].

versus  $-13.9 \text{ kcal}\cdot\text{mol}^{-1}$ ), suggesting that more non-covalent bonds have been formed. However, the enthalpy gain is offset by an equal opposing change in the entropic term ( $-6.9$  versus  $-5.7 \text{ kcal}\cdot\text{mol}^{-1}\cdot\text{K}^{-1}$ ), suggesting that the additional favourable enthalpic interactions have not been matched by desolvation effects, but have added a slight increase in helical propensity. This is in accordance with Agadir and measured helicity (see Table 3), which predicts JunW<sub>CANDI</sub> to have slightly higher helical propensity, contributing to an unfavourable entropic contribution to the free energy of binding.

### cJun(R)–FosW(E)

This designed interaction was generated to investigate the role of electrostatics in the folding of Jun–Fos-based AP-1 coiled coils [15]. The dimer has a significantly enhanced electrostatic ( $g/e$ ) complement. This is of particular interest in aiding future design rounds because we have previously shown it to significantly enhance dimeric stability as the result of a decrease in the dissociation rate of the dimeric complex. In contrast to designing for increased rates of association, this has considerable implications in the design of effective inhibitors. Tailoring the dissociation rate using kinetic design opens up the possibility to increase antagonist efficacy by lengthening the time span that the antagonist–target complex can endure [15,37,38]. The ITC data show that for this dimer there is a very large enthalpic contribution to the interaction stability ( $-27 \text{ kcal}\cdot\text{mol}^{-1}$ ) relative to the other PCA-selected antagonists ( $-10.6$  to  $-14.8 \text{ kcal}\cdot\text{mol}^{-1}$ ) that is, in turn, compensated for by an opposing but comparatively small entropic penalty ( $-17.4 \text{ kcal}\cdot\text{mol}^{-1}\cdot\text{K}^{-1}$ ). The relatively modest helicity for Jun(R) and FosW(E) peptides in isolation, measured by both helicity and Agadir, would appear to suggest that conformational entropy is not a major contributory factor in the efficacy of this dimer. However, the measured helicity of the heterodimer is very high (88%; see Table 3), and is in stark contrast to the helical level predicted from Agadir. This is because, in using Agadir, the helices have been considered in isolation and averaged. However, in reality, the Arg–Glu salt bridges contribute enormously to the integrity of the helical structure via intermolecular electrostatic interactions, and in doing so additionally contribute to a large and favourable enthalpic term. This molecule, therefore, has a large and unfavourable contribution from  $\Delta S_{\text{conf}}$ , in agreement with the high level of measured helicity, and is also likely to have a poor opposing entropic term from  $\Delta S_{\text{solv}}$  because these additional core-flanking electro-

static  $e/g$  interactions are also likely to be heavily solvated. Curiously, although the cJun(R)–FosW(E) dimer is among the most stable of all those measured, the ITC data do not predict the level of stability that was observed from thermal melting data and kinetic folding studies previously reported [14]. However, what is clear is that the magnitudes of the opposing forces are large relative to the other dimers studied and the entropic barrier is surpassed by a strongly opposing enthalpic contribution to give a very stable overall interaction. It is conceivable that less direct methods for determining the thermodynamic stability are not always as reliable as direct thermodynamic methods of measurement such as ITC. This may be particularly true for instances where the enthalpic contribution to binding is significant.

In addition to the predicted levels of helicity from Agadir and the experimentally measured levels from the CD data, we also monitored the ratio between the two minima in ellipticity of the helical CD spectra (see Table 3). Hodges and co-workers [30,31] previously reported that a 222/208 of approximately  $< 0.9$  typically represents an  $\alpha$ -helix, whereas a ratio of  $> 1.0$  is indicative of a stable coiled coil interaction. We note that according to this calculation only FosW and JunW appear to form coiled coiled homodimers, whereas all heterodimers generate ratios that are  $> 0.9$ , except for cJun–cFos (0.75), which is known to have a low binding affinity.

## Discussion

We have used ITC as a tool to dissect the free energy profile into its component parts for the binding of Jun–Fos-based coiled coil dimers. ITC allows the complete thermodynamic characterization of a bimolecular interaction without the need to label or tether. This study included both the wild-type cJun–cFos coiled coil dimer and a range of peptide antagonists that have been designed to bind to and sequester either cJun or cFos. Splitting the free energy of binding into its thermodynamic constituents is important in helping us to elucidate the best way to design for antagonist efficacy. For example, it has been reported that optimizing for the most favourable enthalpic contribution to the free energy of interaction might prove to be a valuable and complementary addition to established tools for selecting and optimizing compounds in lead discovery, owing to the fact that it is a direct method for monitoring the number and/or strength of noncovalent bonds being formed (or broken) between the target and antagonist during complex formation [17]. It has, however, been argued that the enthalpic parameter is also

more difficult to optimize than the entropic contribution to binding, because engineering bonds of the correct length and angle is notoriously difficult to achieve, as is minimizing the degree of interaction between polar groups and the solvent while ensuring that the complex remains in solution. Likewise, it is difficult to overcome enthalpy–entropy compensation, because an engineered gain in enthalpy during bond optimization is often compensated for by entropic loss as the conformation becomes restricted. Thus, complexes in which the binding energy is dominated by a favourable  $\Delta H$  term may be preferred in choosing which to select and take forward for further refinement. Reassuringly, all of our PCA-selected pairs have a strong enthalpic contribution to the free energy of binding, with the entropic component generally disfavoured. Thus, semi-rational design combined with PCA enriches the most efficacious binders by achieving an enthalpically driven antagonist–target interaction. For coiled coils selected from core and electrostatic libraries, a range of intermolecular noncovalent interactions has been selected to optimize the  $\Delta H$  term, with the  $\Delta S$  term appearing to be less essential during the selection

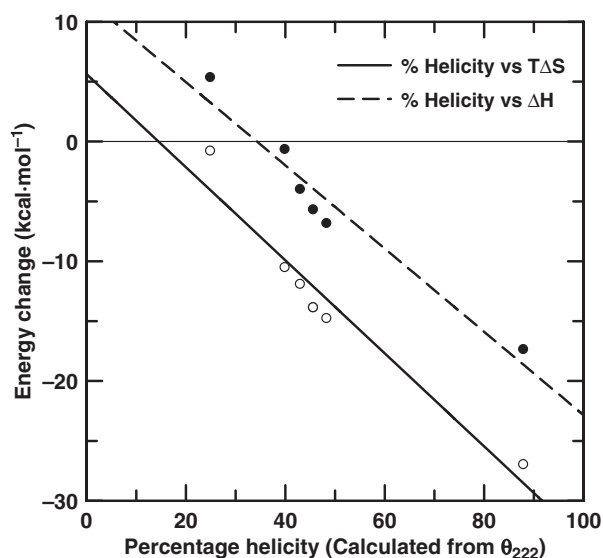


**Fig. 3.** Measured helical percentage plotted against both  $\Delta H$  and  $T\Delta S$  associated with the binding event. Although there are only six data points, both plots reveal a striking relationship ( $r = -0.97$ ) between these two parameters collected from different experiments. The negative gradient indicates that as the helicity of the dimeric pair increases, so too does the entropic penalty because the chains adopt a more ordered conformation. This is more than compensated for by increased enthalpic contributions, which also provide an excellent correlation with measure helicity. The measured helical percentage values are taken from the CD data by using the value in molar residue ellipticity for the minima at 222 nm. The thermodynamic data are derived from ITC.

process. We previously noted that a designed cJun(R)–FosW(E) pair based on cJun–FosW formed a very strong interaction and that the enhanced electrostatics exerted their effect predominantly on the dissociation rate [15]. We speculate that maximizing the enthalpic contribution while reducing the dissociation rate of the antagonist–target complex is an unexplored method for increasing overall binding stability and antagonist efficacy. Finally, we report on the strong correlation ( $r = -0.97$ ) that is observed between the experimentally determined percentage helicity (calculated from the ratio of the observed  $\theta_{222}$  CD minima and the maximal calculated minima possible for a completely helical peptide of same length) and the change in entropy and enthalpy taken from the ITC data (see Fig. 3). Thus, as the measured helicity increases, so does the magnitude of the entropic component that opposes binding. In addition, we observe that as the unfavourable entropic term increases, the contribution made by the enthalpic term also increases, meaning that an equally striking relationship is found between observed helicity and enthalpy, as would be predicted from enthalpy–entropy compensation. The strength of these two relationships suggests that one may be able to monitor the CD spectra of known helical PPIs to assist with the prediction of entropic and enthalpic contributions to the overall binding energy.

The importance of dissecting equilibrium stability to investigate the kinetic contribution to the stability of designed protein–ligand, and particularly protein–drug, interactions is becoming an increasingly recognized area of design [37,38,40]. Further work is required to study the effect of this parameter on PPI specificity, but this study highlights the need for thermodynamic analysis to understand how key PPIs achieve interaction stability and how this information might feed-forward to assist with other parameters in future rounds of protein design. This is likely to be useful in developing peptide and peptidomimetic antagonists for lead discovery in which early identification of hits is likely to vastly accelerate the path to lead discovery [41].

## Experimental procedures

### Protein preparation

Peptides were previously derived by either using semi-rational design and selection with PCA or CANDI-PCA, or were designed based on these previously selected structures. Once the sequence of each peptide antagonist (see Table 1) had been verified by DNA sequencing, they were purchased as >90% pure from Protein Peptide Research Ltd

(Fareham, UK) as Fmoc synthesized and amidated/acetylated and contained N- and C-capping motifs for improved stability and solubility. Peptides were further purified where necessary using reverse-phase HPLC. Peptide concentrations were determined in water using absorbance at 280 nm with an extinction coefficient of  $1209 \text{ M}^{-1}\cdot\text{cm}^{-1}$  [42] corresponding to a Tyr residue inserted into a solvent exposed b3 heptad position.

## ITC measurements

ITC measurements were made using a Microcal VP-ITC instrument and data were collected and processed using the ORIGIN 7.0 software package. All measurements were carried out at least twice. Briefly, all peptides were studied at 20 °C in 10 mM potassium phosphate and 100 mM potassium fluoride at pH 7. Peptide 1 (600 µL) was loaded into the syringe at a concentration between 175 and 250 µM. Peptide 2 (1800 µL) was loaded into the cell at 10–40 µM. The peptide in the syringe and cell were reversed to check that the results were unaffected by this change. The experiment was undertaken by injecting  $5 \mu\text{L} \times 40$  injections of peptide 1 into the calorimetric cell. The change in thermal power as a function of each injection was automatically recorded using Microcal ORIGIN software [39] and the raw data were integrated to yield ITC isotherms of heat release per injection as a function of the Fos to Jun molar ratio. In general, the concentration of peptide 2 loaded into the cell was  $30 \times$  the anticipated PPI  $K_D$  and the concentration of peptide 1 in the syringe was at least  $20 \times$  the concentration of peptide 2. No precipitation of protein was observed in any of the experiments undertaken. Following ITC measurements, the data were fit to a one-site model:

$$q(i) = (n\Delta \text{HVP}/2)[1 + (L/nP) + (K_d/nP)] - \{[1 + (L/nP) + (K_d/nP)]^2 - (4L/nP)\}^{1/2} \quad (2)$$

where  $q(i)$  is the heat release ( $\text{kcal}\cdot\text{mol}^{-1}$ ) for the  $i$ th injection,  $n$  is the stoichiometry of heterodimerization,  $V$  is the effective volume of protein sample loaded into the calorimetric cell (1.46 mL),  $P$  is the total Jun concentration in the calorimetric cell (µM) and  $L$  is the total Fos concentration in the calorimetric cell at the end of each injection (µM). This model is derived from the binding of a ligand to a macromolecule using the law of mass action (assuming a 1 : 1 stoichiometry) to extract the various thermodynamic parameters [18], namely the apparent equilibrium constant ( $K_d$ ) and the enthalpy change ( $\Delta H$ ) associated with heterodimerization. The free energy change ( $\Delta G_{\text{bind}}$ ) upon ligand binding can be calculated from the relationship:

$$\Delta G_{\text{bind}} = -RT \ln K_D \quad (3)$$

where  $R$  is the universal molar gas constant ( $1.9872 \text{ kcal}\cdot\text{mol}^{-1}\cdot\text{K}^{-1}$ ),  $T$  is the absolute temperature in Kelvin (293.15 K) and  $K_D$  is the dissociation constant of binding

with units of  $\text{mol}\cdot\text{L}^{-1}$ . Finally, the entropic contribution ( $T\Delta S$ ) to the free energy of binding was calculated by rearranging Eqn (1) using the derived values of  $\Delta H$  and  $\Delta G_{\text{bind}}$ .

## Acknowledgements

This work was supported by funding from the Wellcome Trust (Grant #DBB2800). In addition, the authors wish to thank the Department of Biological Sciences RCIF funding for the purchase of an isothermal titration calorimeter.

## References

- Ozanne BW, Spence HJ, McGarry LC & Hennigan RF (2007) Transcription factors control invasion: AP-1 the first among equals. *Oncogene* **26**, 1–10.
- Eferl R & Wagner EF (2003) AP-1: a double-edged sword in tumorigenesis. *Nat Rev Cancer* **3**, 859–868.
- Hess J, Angel P & Schorpp-Kistner M (2004) AP-1 subunits: quarrel and harmony among siblings. *J Cell Sci* **117**, 5965–5973.
- Aud D & Peng SL (2006) Mechanisms of disease: transcription factors in inflammatory arthritis. *Nat Clin Pract Rheumatol* **2**, 434–442.
- Wagner EF & Eferl R (2005) Fos/AP-1 proteins in bone and the immune system. *Immunol Rev* **208**, 126–140.
- Zenz R, Eferl R, Scheinecker C, Redlich K, Smolen J, Schonhaler HB, Kenner L, Tschachler E & Wagner EF (2008) Activator protein 1 (Fos/Jun) functions in inflammatory bone and skin disease. *Arthritis Res Ther* **10**, 201.
- Glover JN & Harrison SC (1995) Crystal structure of the heterodimeric bZIP transcription factor c-Fos–c-Jun bound to DNA. *Nature* **373**, 257–261.
- Reinke AW, Grant RA & Keating AE (2010) A synthetic coiled-coil interactome provides heterospecific modules for molecular engineering. *J Am Chem Soc* **132**, 6025–6031.
- Pelletier JN, Arndt KM, Pluckthun A & Michnick SW (1999) An in vivo library-versus-library selection of optimized protein–protein interactions. *Nat Biotechnol* **17**, 683–690.
- Remy I & Michnick SW (1999) Clonal selection and in vivo quantitation of protein interactions with protein-fragment complementation assays. *Proc Natl Acad Sci USA* **96**, 5394–5399.
- Mason JM, Schmitz MA, Muller KM & Arndt KM (2006) Semirational design of Jun–Fos coiled coils with increased affinity: universal implications for leucine zipper prediction and design. *Proc Natl Acad Sci USA* **103**, 8989–8994.
- Mason JM, Muller KM & Arndt KM (2007) Positive aspects of negative design: simultaneous selection of

- specificity and interaction stability. *Biochemistry* **46**, 4804–4814.
- 13 Mason JM, Muller KM & Arndt KM (2008) iPEP: peptides designed and selected for interfering with protein interaction and function. *Biochem Soc Trans* **36**, 1442–1447.
  - 14 Mason JM, Hagemann UB & Arndt KM (2009) Role of hydrophobic and electrostatic interactions in coiled coil stability and specificity. *Biochemistry* **48**, 10380–10388.
  - 15 Mason JM (2009) Electrostatic contacts in the activator protein-1 coiled coil enhance stability predominantly by decreasing the unfolding rate. *FEBS J* **276**, 7305–7318.
  - 16 Lafont V, Armstrong AA, Ohtaka H, Kiso Y, Mario Amzel L & Freire E (2007) Compensating enthalpic and entropic changes hinder binding affinity optimization. *Chem Biol Drug Des* **69**, 413–422.
  - 17 Ladbury JE, Klebe G & Freire E (2010) Adding calorimetric data to decision making in lead discovery: a hot tip. *Nat Rev Drug Discov* **9**, 23–27.
  - 18 Seldeen KL, McDonald CB, Deegan BJ & Farooq A (2008) Thermodynamic analysis of the heterodimerization of leucine zippers of Jun and Fos transcription factors. *Biochem Biophys Res Commun* **375**, 634–638.
  - 19 Seldeen KL, McDonald CB, Deegan BJ & Farooq A (2008) Coupling of folding and DNA-binding in the bZIP domains of Jun–Fos heterodimeric transcription factor. *Arch Biochem Biophys* **473**, 48–60.
  - 20 Mason JM, Muller KM & Arndt KM (2009) peptides tailored to interfere with protein interaction and function. *Chem Today* **27**, 47–50.
  - 21 Mason JM, Hagemann UB & Arndt KM (2007) Improved stability of the Jun–Fos activator protein-1 coiled coil motif: a stopped-flow circular dichroism kinetic analysis. *J Biol Chem* **282**, 23015–23024.
  - 22 Mason JM & Arndt KM (2004) Coiled coil domains: stability, specificity, and biological implications. *Chem-biochem* **5**, 170–176.
  - 23 Woolfson DN (2005) The design of coiled-coil structures and assemblies. *Adv Protein Chem* **70**, 79–112.
  - 24 O'shea EK, Rutkowski R & Kim PS (1992) Mechanism of specificity in the Fos–Jun oncoprotein heterodimer. *Cell* **68**, 699–708.
  - 25 Boysen RI, Jong AJ, Wilce JA, King GF & Hearn MT (2002) Role of interfacial hydrophobic residues in the stabilization of the leucine zipper structures of the transcription factors c-Fos and c-Jun. *J Biol Chem* **277**, 23–31.
  - 26 Patel LR, Curran T & Kerppola TK (1994) Energy transfer analysis of Fos–Jun dimerization and DNA binding. *Proc Natl Acad Sci USA* **91**, 7360–7364.
  - 27 Olive M, Krylov D, Echlin DR, Gardner K, Taparowsky E & Vinson C (1997) A dominant negative to activation protein-1 (API) that abolishes DNA binding and inhibits oncogenesis. *J Biol Chem* **272**, 18586–18594.
  - 28 Newman JR & Keating AE (2003) Comprehensive identification of human bZIP interactions with coiled-coil arrays. *Science* **300**, 2097–2101.
  - 29 Fong JH, Keating AE & Singh M (2004) Predicting specificity in bZIP coiled-coil protein interactions. *Genome Biol* **5**, R11.
  - 30 Lau SY, Taneja AK & Hodges RS (1984) Synthesis of a model protein of defined secondary and quaternary structure. Effect of chain length on the stabilization and formation of two-stranded alpha-helical coiled-coils. *J Biol Chem* **259**, 13253–13261.
  - 31 Kwok SC & Hodges RS (2004) Stabilizing and destabilizing clusters in the hydrophobic core of long two-stranded alpha-helical coiled-coils. *J Biol Chem* **279**, 21576–21588.
  - 32 Chen YH, Yang JT & Chau KH (1974) Determination of the helix and beta form of proteins in aqueous solution by circular dichroism. *Biochemistry* **13**, 3350–3359.
  - 33 Shepherd NE, Hoang HN, Abbenante G & Fairlie DP (2005) Single turn peptide alpha helices with exceptional stability in water. *J Am Chem Soc* **127**, 2974–2983.
  - 34 Munoz V & Serrano L (1995) Elucidating the folding problem of helical peptides using empirical parameters. III. Temperature and pH dependence. *J Mol Biol* **245**, 297–308.
  - 35 Munoz V & Serrano L (1995) Elucidating the folding problem of helical peptides using empirical parameters. II. Helix macrodipole effects and rational modification of the helical content of natural peptides. *J Mol Biol* **245**, 275–296.
  - 36 Munoz V & Serrano L (1994) Elucidating the folding problem of helical peptides using empirical parameters. *Nat Struct Biol* **1**, 399–409.
  - 37 Copeland RA, Pompliano DL & Meek TD (2006) Drug-target residence time and its implications for lead optimization. *Nat Rev Drug Discov* **5**, 730–739.
  - 38 Tummino PJ & Copeland RA (2008) Residence time of receptor–ligand complexes and its effect on biological function. *Biochemistry* **47**, 5481–5492.
  - 39 Wiseman T, Williston S, Brandts JF & Lin LN (1989) Rapid measurement of binding constants and heats of binding using a new titration calorimeter. *Anal Biochem* **179**, 131–137.
  - 40 Zhang R & Monsma F (2009) The importance of drug-target residence time. *Curr Opin Drug Discov Devel* **12**, 488–496.
  - 41 Mason JM (2010) Design and development of peptides and peptide mimetics as antagonists for therapeutic intervention. *Future Med Chem* **2**, 1813–1822.
  - 42 Du H, Fu R, Li J, Corkan A & Lindsey JS (1998) PhotochemCAD: a computer aided design and research tool in photochemistry. *Photochem Photobiol* **68**, 141–142.